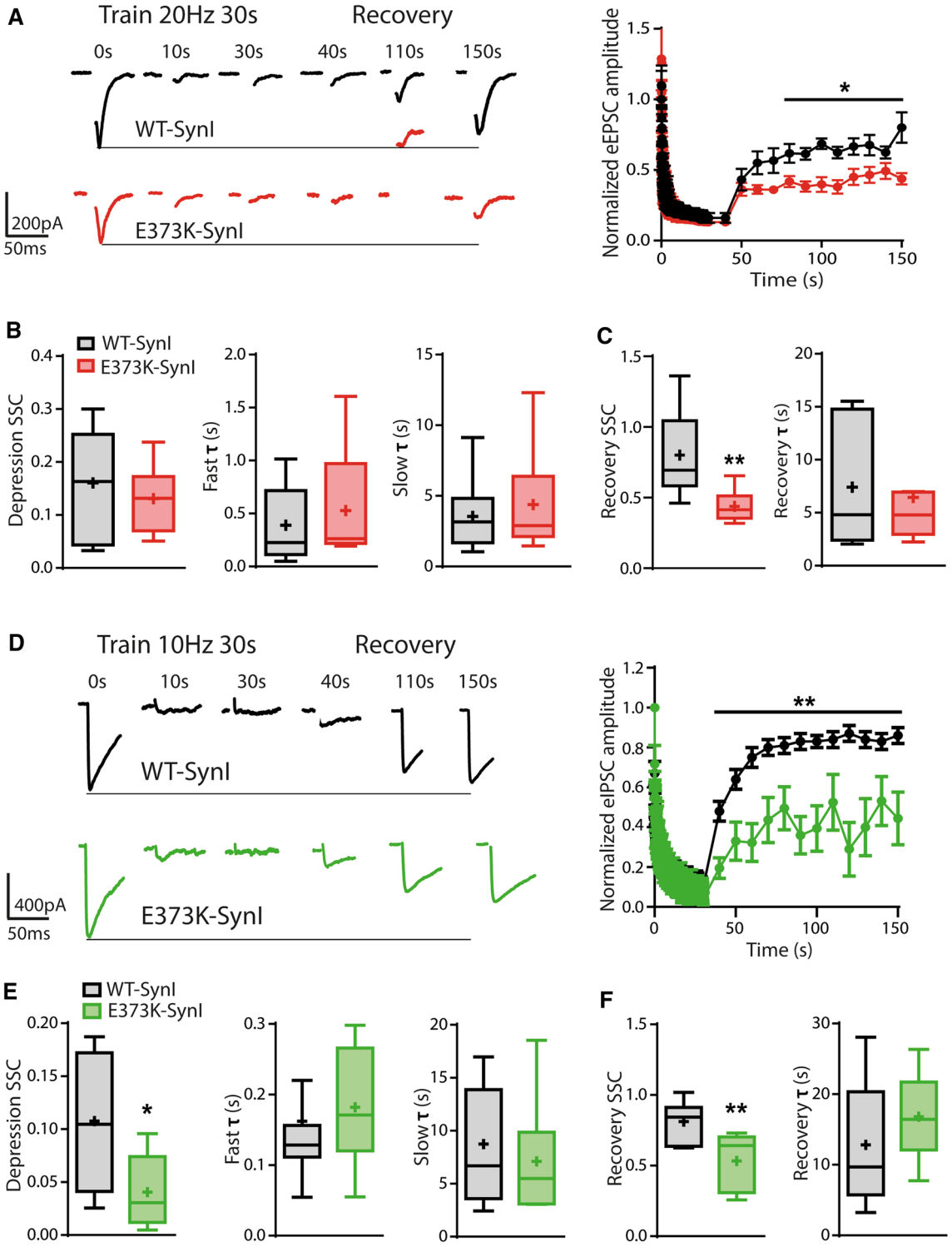

The same cumulative amplitude analysis was performed on inhibitory synapses, using a 40 Hz train for 2.5 s (Fig. 7E). While the decreased eIPSC amplitude of SynI^{KO} synapses was associated with a corresponding decrease in the RRP_{syn}, as previously reported [14], the lack of effect of SynI^{E373K} on the eIPSC amplitude was confirmed by the absence of significant changes in the quantal parameters of synchronous inhibitory transmission (Fig. 7F). Taken together, the data suggest that the SynI^{E373K} mutant affects the activity-dependent refilling of the RRP from the RecP specifically in excitatory synapses.

◂**Fig. 8** The $SynI^{E373K}$ mutant impairs recovery from depression in both excitatory and inhibitory synapses. **A**–**C** Excitatory synapses. Excitatory SynI KO autaptic neurons were transduced with either $SynI^{WT}$ (black) or $SynI^{E373K}$ (red). **A** *Left:* Representative traces of eEPSCs evoked by stimulating neurons with high-frequency trains lasting 30 s at 20 Hz. *Right:* The progressive decay of the eEPSC amplitude (means ± SEM) during the stimulation train and the subsequent recovery from depression upon return of the stimulation frequency to 0.1 Hz are plotted as a function of time from the beginning of the train ($n = 9$ and 8 for $SynI^{WT}$ and $SynI^{E373K}$, respectively). **B** Box plots of the depression steady-state current (SSC, *left*) and of the fast (*middle*) and slow (*right*) time constants of depression (τ). **C** Box plots of the SSC (*left*) and τ (*right*) of recovery after the stimulation train. **D**–**F** Inhibitory synapses. Inhibitory SynI KO neurons were transduced with either $SynI^{WT}$ (black) or $SynI^{E373K}$ (green). **D** *Left:* Representative traces of eIPSCs evoked by stimulating neurons for 30 s at 20 Hz. *Right:* The progressive decay of the eIPSC amplitude (means ± SEM) during the stimulation train and the recovery from depression are plotted as a function of time ($n = 9$ and 8 for $SynI^{WT}$ and $SynI^{E373K}$, respectively). (**E**) Box plots of the depression steady-state current (SSC, *left*) and of the fast (*middle*) and slow (*right*) time constants of depression (τ). (**F**) Box plots of the SSC (*left*) and τ (*right*) of recovery after the stimulation train. Data are from $n = 3$ independent neuronal preparations. $*p < 0.05$; $**p < 0.01$; Mann–Whitney *U*-test (**A**) or unpaired Student's *t*-test (**C**–**F**)

$SynI^{E373K}$ impairs the recovery from synaptic depression in both excitatory and inhibitory synapses

Central synapses in mice lacking one or more Syn isoforms display a marked decrease in SV density, reflecting a depletion of the RecP and changes in short-term, but not long-term, synaptic plasticity [34, 48, 69, 70, 76, 78, 80]. Accordingly, most of the available data indicate that Syn deletion enhances synaptic depression during repetitive stimulation [25, 34]. Excitatory and inhibitory synapses of SynI KO neurons transduced with either $SynI^{WT}$ or $SynI^{E373K}$ were subjected to a prolonged high-frequency stimulation (HFS). The progressive decay of the ePSCs amplitude during the train and the subsequent recovery from depression upon returning the stimulation frequency to 0.1 Hz were exponentially fitted and analyzed for the kinetic parameters and the steady-state current of depression and recovery. During sustained HFS (30 s @ 20 Hz), $SynI^{E373K}$ excitatory synapses presented no significant changes in the depression steady-state current (SSC) and in the slow and fast time constants of depression (Fig. 8A, B). However, they showed a significant impairment in the recovery after depression with an almost two-fold difference in the recovery SSC with respect to $SynI^{WT}$, in the absence of changes in the time constant of recovery (Fig. 8A, C). Under sustained HFS (30 s @ 10 Hz), $SynI^{E373K}$ inhibitory synapses showed a significantly lower depression SSC than $SynI^{WT}$ inhibitory synapses, with no significant differences in the slow and fast time constants of depression (Fig. 8D, E). In addition, inhibitory synapses displayed an impaired recovery after depression similar to that observed at excitatory synapses: the first response after the stimulus train was markedly smaller than in $SynI^{WT}$ synapses and the recovery SSC was twofold lower, with no change in the time constant of recovery (Fig. 8D, F).

These results suggest that the $SynI^{E373K}$ mutant strongly impairs the recovery from depression in both excitatory and inhibitory synapses and the steady state of depression in inhibitory synapses. This suggests that Ca^{2+} binding to SynI plays a role in the dynamics of SV pools and in SV mobilization during and after sustained HFS in both types of synapses.

$SynI^{E373K}$ impairs SV recycling and slows-down the kinetics of RRP refilling

To further investigate the mechanisms of defective recovery after the stimulus in $SynI^{E373K}$ synapses, we performed synaptophysin-pHluorin (sypHy)-based live cell imaging experiments. Primary SynI KO hippocampal neurons were co-transduced at 10 DIV with lentiviral vectors encoding sypHy and either $SynI^{WT}$ or $SynI^{E373K}$ fused to mCherry and analyzed 8–11 days after transduction (Fig. 9A).

We first evaluated the RRP, which in synaptic imaging accounts for both synchronous and asynchronous components of releasable SVs, by stimulating neurons with 20 APs @100 Hz [4]. While no genotype-dependent differences were present in the peak fluorescence, a significant increase in the time constant of fluorescence decay was observed in $SynI^{E373K}$ as compared to $SynI^{WT}$ terminals, revealing an impaired SV endocytosis, suggestive of defective recovery after RRP depletion (Fig. 9B). The lack of change in the RRP measured by sypHy imaging suggests that the decreased RRP_{syn} observed by patch-clamp recordings (see Fig. 7B) is accompanied by an increase of asynchronous release that may be facilitated by the increased resting Ca^{2+} (see Fig. 4). Next, to measure recovery after sustained stimulation, we performed repetitive RRP stimulations (20 APs @ 100 Hz) before or after a long-lasting stimulation (600 APs @ 20 Hz; Fig. 9C). Consecutive RRP stimuli resulted in a mild and not significant rundown in both $SynI^{WT}$ and $SynI^{E373K}$ synapses. Despite the peak fluorescence evoked by the first round of stimulation was not changed between the two genotypes, the RRP after the long-lasting stimulation was significantly reduced in $SynI^{E373K}$ synapses (Fig. 9C). These data confirmed the defective SV recovery after sustained stimulation in $SynI^{E373K}$ neurons.

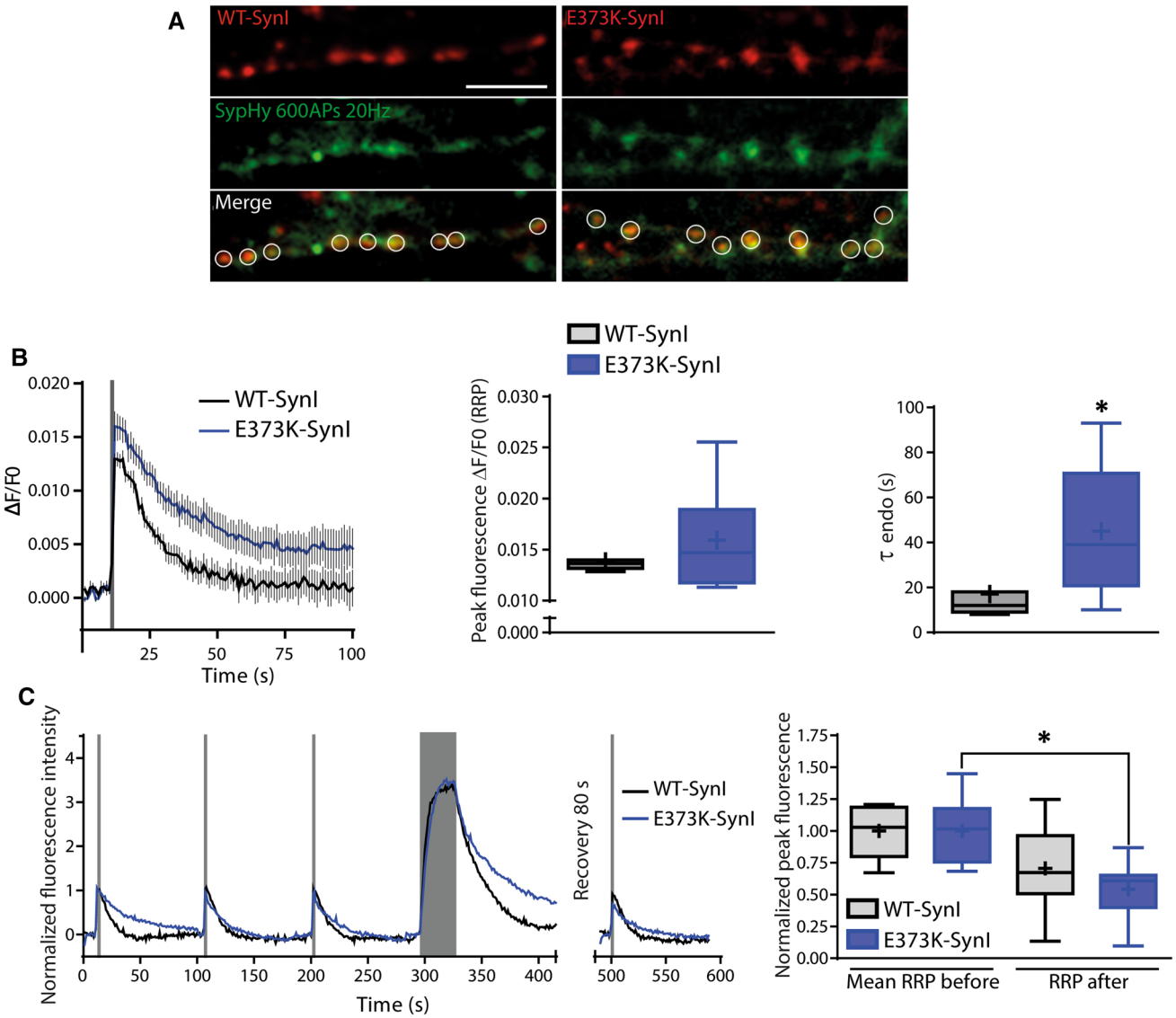

Fig. 9 The recovery from the synaptic activity is altered in nerve terminals expressing the SynI^{E373K} mutant. **A** Representative images showing axonal branches from 21 DIV SynI KO hippocampal neurons transduced with sypHy (green) and either Syn^{WT} (*left*) or SynI^{E373K} (*right*) fused to mCherry (red) during a 600 AP stimulation @ 20 Hz. White regions of interest (ROI) label co-transduced synapses. Scale bar, 3 µm. **B** *Left:* Ensemble average traces of sypHy fluorescence plotted for Syn^{WT} (black) and SynI^{E373K} (blue). Stimulation (20 APs@100 Hz) is indicated by the gray bar. Data are means ± SEM of $n = 7$ and 11 coverslips for Syn^{WT} and SynI^{E373K}, respectively. *Middle:* Box plot of peak fluorescence at the end of the stimulus in the two genotypes. *Right:* Box plot of time constant of endocytosis (τ_{endo}), evaluated by fitting the fluorescence decay after stimulation with a mono-exponential function. $^*p < 0.05$, Mann–Whitney's *U*-test. **C** *Left:* Representative traces from Syn^{WT} (black) and SynI^{E373K} (blue) expressing synapses stimulated with three RRP trains (20 APs@100 Hz, thin gray bars), subjected to a long-lasting stimulation (600 APs@20 Hz, thick gray bar) and challenged with a further RRP stimulation. Traces were normalized to the first stimulus. *Right:* Box plot showing the average peak fluorescence for the three consecutive RRP stimulations before the long-lasting train, and the response to an additional RRP stimulation performed after the long-lasting train. Data are from $n = 9$ coverslips per genotype. $^*p < 0.05$, one-way ANOVA/Tukey's tests

Ultrastructural analysis reveals that $SynI^{E373K}$ affects SV trafficking at rest and during activity

To verify if the defects in the excitatory RRP_{syn} and recovery from synaptic depression in both excitatory and inhibitory synapses were due to alterations in SV trafficking, we evaluated the density and distribution of SVs in presynaptic terminals by electron microscopy of "asymmetric" (i.e., excitatory) and "symmetric" (i.e., inhibitory) synapses expressing either $SynI^{WT}$ or $SynI^{E373K}$.

Transduced excitatory and inhibitory synapses were analyzed at rest (1 s before the stimulation train) and at the following HFS (30 s @ 20 Hz) by quickly fixing the samples at the end of train and during the recovery period (2 min after the train) (Fig. 10A, C). At rest, excitatory $SynI^{E373K}$ synapses showed a significant reduction in total SV density with respect to control $SynI^{WT}$ synapses (Fig. 10B; *left panel*). Although no genotype-dependent changes were detected in the density of physically docked SVs (Fig. 10B; *right panel*), the decreased SV content is consistent with an impaired RRP refilling in mutant nerve terminals that could account for the functionally determined decrease in RRP_{syn} (see Fig. 7B). The total SV density was decreased under the condition of deep synaptic depression reached at the end of the stimulation train, but with no apparent genotype-dependent differences. However, at the end of the recovery period, excitatory synapses failed to recover the basal SV density (Fig. 10B; *left panel*), recapitulating the defective recovery evaluated electrophysiologically (see Fig. 8A). At rest and the end of the stimulation train, inhibitory $SynI^{E373K}$ synapses were closely similar to control $SynI^{WT}$ synapses in terms of total and docked SV densities (Fig. 10D). However, similarly to excitatory synapses, the total SV density of mutant inhibitory terminals failed to recover the basal SV density, consistent with the electrophysiological data (Fig. 10D; *left panel*).

Taken together, these results show that the absence of Ca^{2+} binding to SynI mainly affects excitatory synapses that fail to maintain a correct distribution of SVs under basal conditions. Moreover, in both excitatory and inhibitory synapses, the deletion of the Ca^{2+} binding site dysregulates the SynI-mediated trafficking of SVs in terminals challenged with sustained HFS.

Discussion

Genetic analyses in human populations have identified several mutations in the *SYN1* and *SYN2* genes related to epilepsy and autism spectrum disorder [1, 17, 27, 31, 60, 65, 84], for a review, see [38]. Moreover, several studies of single and multiple Syn KO mice models confirmed the relationship between the *Syn1/Syn2* genes, epilepsy, and autism [16, 26, 35, 48, 55, 70]. Thus, the study of the precise functional role of Syns in excitatory and inhibitory synapses and their structure–function relationships within nerve terminals is fundamental to understanding the pathogenesis of such diseases.

SynI is present in nerve terminals at an average concentration of about 10–20 μM. It represents the 4% of SV proteins and 8–10 copies of SynI are associated with a single SV [20, 72, 79]. The crystal structure of the highly conserved central C-domain of SynI revealed a binding site for ATP, formed by a flexible MFL loop (residues 330–343), with high similarity with "ATP-grasp" enzymes [23]. In the proximity of the ATP binding site, SynI binds Ca^{2+} by coordinating it with the pyrophosphate moiety of ATP and two glutamate residues (Glu373 and Glu386). Structural studies and biochemical data on recombinant Syns suggested the possibility that ATP binding is regulated by Ca^{2+} [39]. Notwithstanding these data, the role of ATP binding to SynI and SynII has remained elusive. Based on the crystal structure of domain C, an increase in SynI tetramer formation upon binding of ATP in the presence of Ca^{2+} was reported [10]. More recently, using MD simulations and biochemical assays, we found that the MFL loop has a similarly reduced motility to holo-SynI also in the absence of Ca^{2+} and, consistently, SynI can bind ATP also in the absence of Ca^{2+} [62]. We also found that ATP binding strengthens the SynI association with SVs, favors the formation of high-order dimers and tetramers, and increases SV clustering. Under these conditions, the presence of Ca^{2+} negatively modulates SV clustering and favors the formation of tetramers over that of dimers [62] consistent with the previous structural predictions [10].

Deletion of ATP binding in SynI induced an increase in the probability of release at inhibitory synapses that potentiated the responses to single stimulation and increased synaptic depression [62]. Deletion of the same site in SynII also increased the probability of release and synaptic depression at excitatory synapses [75]. Although the two studies were done in distinct types of synapses, they show a similar functional outcome of the ATP binding site deletion in both Syn isoforms irrespective of the presence of Ca^{2+} binding, indicating the existence of distinct roles for Ca^{2+} and ATP binding to SynI/SynII. Since the micromolar ATP concentrations in nerve terminals do not represent a limiting factor for protein binding [67], it has so far been difficult to investigate separately the role of ATP binding to SynI from that of Ca^{2+} binding, and no specific role for Ca^{2+} binding to SynI has been proposed, except for facilitating ATP binding. Here, we show that ATP and Ca^{2+} binding by the SynI C-domain are independent events that, however, cooperatively potentiate each other. Thus, Ca^{2+} enhances ATP binding and, conversely, ATP increases the strength of Ca^{2+}binding to SynI. To dissect out the physiological role of Ca^{2+} binding to SynI, we analyzed the effects of the E373K mutation that deletes the major Ca^{2+}

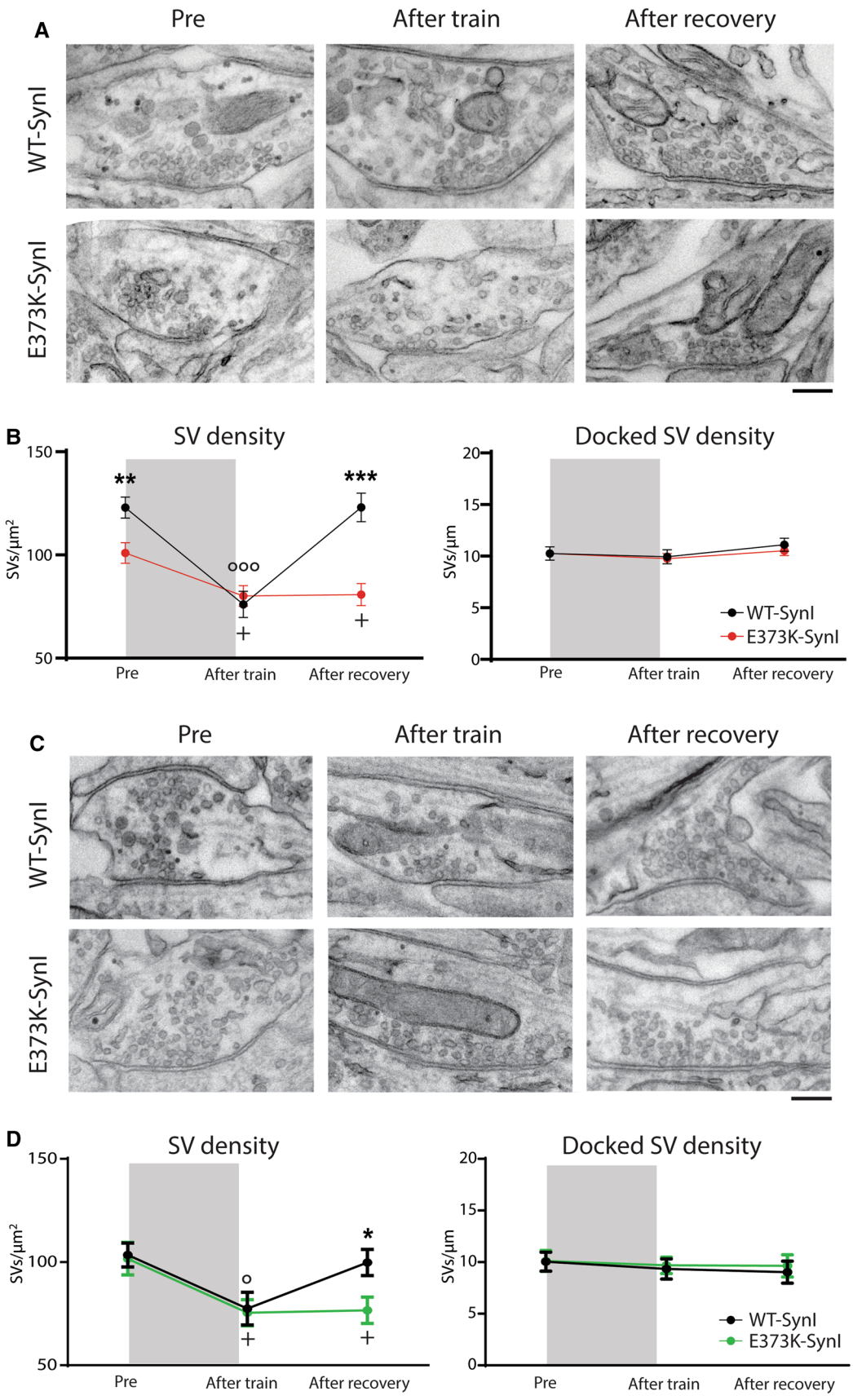
A
Pre
After train
After recovery
WT-Synl
E373K-Synl
B
SV density
SVs/µm²
150
100
50
**
***
ooo
+
+
Pre
After train
After recovery
Docked SV density
SVs/µm
20
15
10
5
0
WT-Synl
E373K-Synl
C
Pre
After train
After recovery
WT-Synl
E373K-Synl
D
SV density
SVs/µm²
150
100
50
*
o
+
+
Pre
After train
After recovery
Docked SV density
SVs/µm
20
15
10
5
0
WT-Synl
E373K-Synl

◂**Fig. 10** SV density and distribution are altered in excitatory and inhibitory synapses expressing the $SynI^{E373K}$ mutant. **A, B** Excitatory synapses. **A** Representative transmission electron micrographs of excitatory presynaptic terminals from SynI KO neurons transduced with either $SynI^{WT}$ (top) or $SynI^{E373K}$ (bottom) and rapidly (1 s) fixed under resting conditions (*Pre*), immediately after a 30 s tetanic stimulation @ 20 Hz (*After train*) and following 120 s of recovery (*After recovery*). Scale bar, 200 nm. **B** Morphometric analysis of excitatory presynaptic terminals. For each genotype and experimental condition, the total SV density (*left*) and the number of docked SVs (*right*) are shown as means ± SEM. **C**, **D** Inhibitory synapses. **C** Representative transmission electron micrographs of inhibitory presynaptic terminals quickly fixed under the conditions as described in **A**. Scale bar, 200 nm. **D** Morphometric analysis of inhibitory presynaptic terminals. The total SV density (*left*) and the number of docked SVs (*right*) are shown for each genotype and experimental condition as means ± SEM. Excitatory and inhibitory synapses were manually identified based on their asymmetric or symmetric shape. Excitatory synapses: $n = 30$ and 30; inhibitory synapses: $n = 15$ and 15; for $SynI^{WT}$ and $SynI^{E373K}$, respectively, from 2 independent neuronal preparations. Across genotype: $^{*}p < 0.05$; $^{**}p < 0.01$; $^{***}p < 0.001$; unpaired Student's *t*-test. Within genotype: $^{\circ}p < 0.05$; $^{\circ\circ\circ}p < 0.001$; *vs* "*Pre*" for $SynI^{WT}$; $^{+}p < 0.05$ *vs* "*Pre*" for $SynI^{E373K}$; one-way ANOVA/Dunnett's multiple comparison test

binding site in SynI and induces a destabilization of the SynI oligomerization interface that is not dissimilar to that observed after deletion of the ATP binding site [62].

We found that the ablation of the Ca^{2+} binding in SynI had more severe consequences in excitatory than in inhibitory synapses. In the former synapses, the deletion of SynI-Ca^{2+} binding increased the frequency of mEPSCs without altering synaptic density and decreased the EPSC amplitude evoked by single stimuli. Distinct, but related, mechanisms are involved in these two effects. Under physiological conditions, SynI may act as a Ca^{2+} buffer, regulating the concentration of this ion in the presynaptic compartment. In the absence of Ca^{2+} sequestration by SynI, the resting Ca^{2+} concentration in excitatory nerve terminals could increase sufficiently to enhance spontaneous SV exocytosis that generates miniature events. Indeed, although the spontaneous release is independent of action potentials, it is at least partly Ca^{2+}-dependent [44, 45, 59, 77]. This hypothesis is further confirmed by the observation that supplementation of an exogenous Ca^{2+} buffer completely occluded the effect of the SynI mutant. Why a similar effect is not occurring in inhibitory synapses that also express, to a large extent, SynI [9]? One possible explanation is that inhibitory neurons express a variety of Ca^{2+}-buffering proteins [74], such as parvalbumin, calbindin, and calretinin [3, 22, 37, 41, 46, 77, 81] that characterize their peculiar functional properties. Under these conditions, the expression of Ca^{2+}-buffering proteins by distinct classes of interneurons may render the contribution of the SynI-mediated buffering dispensable under resting conditions. It will be interesting to investigate whether the expression of parvalbumin in excitatory neurons occludes the effect of $SynI^{E373K}$ mutation or, alternatively, whether silencing endogenous Ca^{2+} buffers in inhibitory neurons makes them sensitive to the E373K mutation.

On the other hand, the decreased EPSC amplitude due to a selective decrease in RRP size can be a consequence of the decreased SV density observed by electron microscopy in excitatory synapses under resting conditions. Although we did not detect any change in the density of physically docked SVs, the decrease in RRP can be explained by a decreased refilling with primed SVs from a more dispersed RecP. Such dispersion can be a consequence of: (i) the increased resting intraterminal Ca^{2+} that stimulates CaM kinases to phosphorylate SynI, favoring the release of SVs from the clusters and the actin cytoskeleton; and/or (ii) a possible mutation-induced change in SynI oligomerization, as suggested by MD simulations, that may alter the SV clustering capacity. Recent work demonstrated the capability of Syns to trigger liquid phase separation that participates in the clustering and maintenance of the SV pools in nerve terminals [57, 58, 64] and that is released upon Syn phosphorylation by CaM kinases [58]. Thus, a tonic activation of CaM kinases due to the increased concentration of resting Ca^{2+} could also impair SynI liquid phase separation and lead to SV cluster dispersion. While the deletion of the Ca^{2+} binding site in SynI can be defined as a loss-of-function, some of the phenotypes of $SynI^{E373K}$ appear as gain-of-function when compared to $SynI^{WT}$ and $SynI^{KO}$. Indeed, $SynI^{E373K}$ induces an increase in mEPSC frequency, as the consequence of the increase in resting free Ca^{2+}, while constitutive depletion of SynI does not affect mEPSC frequency or amplitude [14]. On the other hand, constitutive deletion of SynI increases eEPSC amplitude and RRP size as a secondary effect of the impairment in inhibitory transmission [14, 25, 82], while $SynI^{E373K}$ behaves similarly to $SynI^{WT}$, indicating that the RRP size does not depend on Ca^{2+} binding to SynI.

Another effect of the deletion of Ca^{2+}-binding to SynI, shared by excitatory and inhibitory synapses, consists of a sharp impairment in recovering PSCs after prolonged HFS. This effect finds its ultrastructural counterpart in a marked depletion of SVs at the end of the recovery period, indicating a defective RRP refilling. This effect, together with the impaired and slowed down retrieval of exocytosed SVs, suggests a modulation exerted by Ca^{2+} binding on the kinetics of endocytosis that could be mediated by the previously reported interactions of SynI with endocytic proteins such as intersectin and amphiphysin [24, 32, 61]. While all the remaining effects of the Syn mutant were exclusively found in facilitating excitatory synapses, the effects on recovery from depression also extended to an inhibitory transmission that is more prone to experience depression given its higher probability of release.

The putative events triggered by the deletion of Ca^{2+} binding to SynI in excitatory synapses are schematically represented in Fig. 11. Inability to bind Ca^{2+} increases the

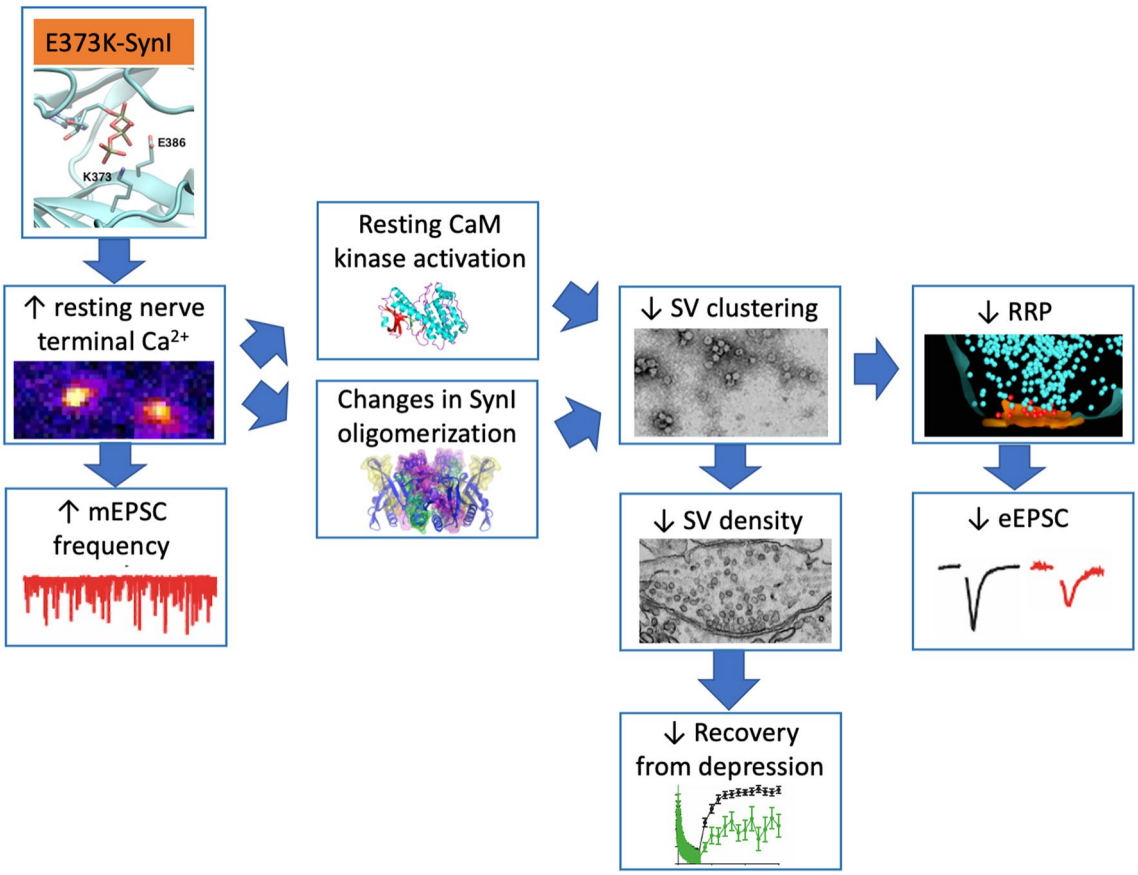

Fig. 11 Schematic model of the functional consequences of the lack of Ca^{2+}-binding to SynI in excitatory synapses. The lack of Ca^{2+}-buffering by SynI in excitatory synapses, characterized by a low Ca^{2+}-buffering capacity, results in an increased intraterminal $[Ca^{2+}]_i$ under resting conditions. This increases the probability of spontaneous SV fusion events and decreases the clustering of SVs in the RecP. This results in a decrease in RRP size for synchronous release and an impairment of the reconstitution of SV stores during recovery after HFS. The decrease in SV clustering may be contributed by an increased tetramerization of SynI and/or to increased phosphorylation of SynI by CaM kinases induced by the rise of resting intraterminal $[Ca^{2+}]_i$. Inhibitory synapses, endowed with a more efficient Ca^{2+}-buffering capacity, are only affected by the lack of Ca^{2+}-buffering by SynI under the intense Ca^{2+} build-up that occurs during HFS

resting Ca^{2+} concentrations which, in turn, increases the frequency of mEPSCs and constitutively activates CaM kinases phosphorylating SynI at distinct sites and promoting its dissociation from SVs and actin. This will in turn reduce SV clustering and disperse SVs in the RecP. The impaired SV clustering may be also contributed by the effect of the mutation on SynI oligomerization [62]. The dispersion of SVs in the RecP can, in turn, be responsible for the decreased RRP-syn and eEPSC amplitude, possibly due to a decreased SV priming and/or refilling of RRP, and for the marked impairment of EPSC recovery after prolonged HFS.

For the time being, the E373K mutation has not been identified in the *SYN1* gene of patients suffering from autism spectrum disorders or epilepsy. The first nonsense mutation in *SYN1* to be reported (W356X; [31] also deletes the Ca^{2+} binding site; however, the expression of the truncated form of synapsin I was markedly impaired, due to both the strongly decreased translation by non-sense mediated RNA decay (NMD) and severe intracellular aggregation of the NMD-escaped protein [33].

In conclusion, we have shown that Ca^{2+} binding to SynI is fundamental for maintaining a physiological SV organization at rest and during/after HFS. Excitatory neurons seem to be more sensitive to the Ca^{2+}-dependent activity of SynI, indicating a putative role of SynI as Ca^{2+} buffer in these terminals under resting conditions. These findings contribute to the clarification of the distinct roles of ATP and Ca^{2+} binding to the highly conserved central C-domain of Syns and underline the central role of the regulation of Ca^{2+} basal levels and transients in nerve terminals in driving SV trafficking, synaptic transmission, and plasticity.

Acknowledgements We thank Dr. Anneke Verstegen (Istituto Italiano di Tecnologia, Genova, Italy) for the generation of the mutant SYN1 cDNA; prof. Luigi Naldini (Tiget, Milano, Italy) for kindly providing the lentiviral plasmids; the Viral Core Facility of Charité (Universitätsmedizin Berlin, Germany) (for the supply of the SynGCaMP6 viral vector; Drs. Riccardo Navone, Arta Mehilli, and Diego Moruzzo (Istituto Italiano di Tecnologia, Genova, Italy) for their help in the maintenance, breeding, and genotyping of the SynI KO mouse strain.

Author contributions MM, GL and TR performed and analyzed the electrophysiological experiments; SC prepared the low-density and autaptic neuronal cultures; MO and ADF performed and analyzed the electron microscopy experiments; DA performed live imaging experiments; LM performed and analyzed MD simulations; AF planned and supervised the live imaging experiments; PB, supervised the electrophysiological experiments and data analysis; FB planned and funded the research, contributed to data analysis and interpretation and wrote the paper.

Funding Open access funding provided by Istituto Italiano di Tecnologia within the CRUI-CARE Agreement. The study was supported by research grants from Compagnia di San Paolo Torino (2015.0546 and 2020.34760 to FB and 2017.20612 to PB); IRCCS Ospedale Policlinico San Martino (Ricerca Corrente and "5 × 1000" to PB and FB) and Italian Ministry of University and Research (PRIN 2015-H4K2CR and 2017-A9MK4R to FB). The support of Telethon-Italy (Grant GGP19120 to FB) is also acknowledged.

Availability of data and material The data and material that support the findings of this study are available upon request to the corresponding authors.

Declarations

Conflict of interest The authors have no relevant financial or non-financial interests to disclose.

Ethics approval All experiments were carried out in accordance with the guidelines established by the European Community Council (Directive 2010/63/EU of 22 September 2010) and were approved by the Italian Ministry of Health (authorization n. 605/2021-PR).

Consent to participate Not applicable.

Consent for publication Not applicable.

References

1. Accogli A, Wiegand G, Scala M, Cerminara C, Iacomino M, Riva A, Carlini B, Camerota L, Belcastro V, Prontera P, Fernández-Jaén A, Bebek N, Scudieri P, Baldassari S, Salpietro V, Novelli G, De Luca C, von Stülpnagel C, Kluger F, Kluger GJ, Wohlrab GC, Ramantani G, Lewis-Smith D, Thomas RH, Lai M, Verrotti A, Striano S, Depienne C, Minetti C, Benfenati F, Brancati F, Zara F, Striano P (2021) Clinical and genetic features in patients with reflex bathing epilepsy. Neurology 97:e577–e586
2. Alabi AA, Tsien RW (2012) Synaptic vesicle pools and dynamics. Cold Spring Harb Perspect Biol 4:a013680
3. Aponte Y, Bischofberger J, Jonas P (2008) Efficient Ca^{2+} buffering in fast-spiking basket cells of rat hippocampus. J Physiol 586:2061–2075
4. Ariel P, Ryan TA (2010) Optical mapping of release properties in synapses. Front Neural Circuits 4:18
5. Baldelli P, Fassio A, Valtorta F, Benfenati F (2007) Lack of synapsin I reduces the readily releasable pool of synaptic vesicles at central inhibitory synapses. J Neurosci 27:13520–13531
6. Bekkers JM, Stevens CF (1991) Excitatory and inhibitory autaptic currents in isolated hippocampal neurons maintained in cell culture. Proc Natl Acad Sci USA 88:7834–7838
7. Benfenati F, Valtorta F, Chieregatti E, Greengard P (1992) Interaction of free and synaptic vesicle-bound synapsin I with F-actin. Neuron 8:377–386
8. Benfenati F, Valtorta F, Rossi MC, Onofri F, Sihra T, Greengard P (1993) Interactions of synapsin I with phospholipids: possible role in synaptic vesicle clustering and in the maintenance of bilayer structures. J Cell Biol 123:1845–1855
9. Bragina L, Candiracci C, Barbaresi P, Giovedì S, Benfenati F, Conti F (2007) Heterogeneity of glutamatergic and GABAergic release machinery in cerebral cortex. Neuroscience 146:1829–1840
10. Brautigam CA, Chelliah Y, Deisenhofer J (2004) Tetramerization and ATP binding by a protein comprising the A, B, and C domains of rat synapsin I. J Biol Chem 279:11948–11956
11. Cesca F, Baldelli P, Valtorta F, Benfenati F (2010) The synapsins: key actors of synapse function and plasticity. Prog Neurobiol 91:313–348
12. Chi P, Greengard P, Ryan TA (2001) Synapsin dispersion and reclustering during synaptic activity. Nat Neurosci 4:1187–1193
13. Chi P, Greengard P, Ryan TA (2003) Synaptic vesicle mobilization is regulated by distinct synapsin I phosphorylation pathways at different frequencies. Neuron 38:68–78
14. Chiappalone M, Casagrande S, Tedesco M, Valtorta F, Baldelli P, Martinoia S, Benfenati F (2009) Opposite changes in glutamatergic and GABAergic transmission underlie the diffuse hyperexcitability of synapsin I-deficient cortical networks. Cereb Cortex 19:1422–1439
15. Coombs ID, Soto D, McGee TP, Gold MG, Farrant M, Cull-Candy SG (2019) Homomeric GluA2(R) AMPA receptors can conduct when desensitized. Nat Commun 10:4312
16. Corradi A, Zanardi A, Giacomini C, Onofri F, Valtorta F, Zoli M, Benfenati F (2008) Synapsin I and synapsin II null mice display an increased age-dependent cognitive impairment. J Cell Sci 121:3042–3051
17. Corradi A, Fadda M, Piton A, Patry L, Marte A, Rossi P, Cadieux-Dion M, Gauthier J, Lapointe L, Mottron L, Valtorta F, Rouleau GA, Fassio A, Benfenati F, Cossette P (2014) SYN2 is an autism predisposing gene: loss-of-function mutations alter synaptic vesicle cycling and axon outgrowth. Hum Mol Genet 23:90–103
18. Crawford DC, Kavalali ET (2015) Molecular underpinnings of synaptic vesicle pool heterogeneity. Traffic 16:338–364

19. Darden T, York D, Pedersen L (1993) Particle mesh Ewald: a Nlog(N) method for Ewald sums in large systems. J Chem Phys 98:10089–10092
20. De Camilli P, Benfenati F, Valtorta F, Greengard P (1990) The synapsins. Annu Rev Cell Biol 6:433–460
21. De Palma M, Naldini L (2002) Transduction of a gene expression cassette using advanced generation lentiviral vectors. Methods Enzymol 346:514–529
22. Eggermann E, Jonas P (2012) How the 'slow' Ca^{2+} buffer parvalbumin affects transmitter release in nanodomain-coupling regimes. Nat Neurosci 15:20–22
23. Esser L, Wang CR, Hosaka M, Smagula CS, Südhof TC, Deisenhofer J (1998) Synapsin I is structurally similar to ATP-utilizing enzymes. EMBO J 17:977–984
24. Evergren E, Benfenati F, Shupliakov O (2007) The synapsin cycle: a view from the synaptic endocytic zone. J Neurosci Res 85:2648–2656
25. Farisello P, Boido D, Nieus T, Medrihan L, Cesca F, Valtorta F, Baldelli P, Benfenati F (2013) Synaptic and extrasynaptic origin of the excitation/inhibition imbalance in the hippocampus of 785 synapsin I/II/III knockout mice. Cereb Cortex 23:581–593
26. Fassio A, Raimondi A, Lignani G, Benfenati F, Baldelli P (2011) Synapsins: from synapse to network hyperexcitability and epilepsy. Semin Cell Dev Biol 22:408–415
27. Fassio A, Patry L, Congia S, Onofri F, Piton A, Gauthier J, Pozzi D, Messa M, Defranchi E, Fadda M, Corradi A, Baldelli P, Lapointe L, St-Onge J, Meloche C, Mottron L, Valtorta F, Khoa Nguyen D, Rouleau GA, Benfenati F, Cossette P (2011) SYN1 loss-of-function mutations in autism and partial epilepsy cause impaired synaptic function. Hum Mol Genet 20:2297–2307
28. Fornasiero EF, Bonanomi D, Benfenati F, Valtorta F (2010) The role of synapsins in neuronal development. Cell Mol Life Sci 67:1383–1396
29. Forte N, Binda F, Contestabile A, Benfenati F, Baldelli P (2020) Synapsin I synchronizes GABA release in distinct interneuron subpopulations. Cereb Cortex 30:1393–1406
30. Frenkel D, Smit B (2001) Understanding molecular simulation: from algorithms to applications, 2nd edn. Academic Press, San Diego
31. Garcia CC, Blair HJ, Seager M, Coulthard A, Tennant S, Buddles M, Curtis A, Goodship JA (2004) Identification of a mutation in synapsin I, a synaptic vesicle protein, in a family with epilepsy. J Med Genet 41:183–186
32. Gerth F, Jäpel M, Pechstein A, Kochlamazashvili G, Lehmann M, Puchkov D, Onofri F, Benfenati F, Nikonenko AG, Fredrich K, Shupliakov O, Maritzen T, Freund C, Haucke V (2017) Intersectin associates with synapsin and regulates its nanoscale localization and function. Proc Natl Acad Sci USA 114:12057–12062
33. Giannandrea M, Guarnieri FC, Gehring NH, Monzani E, Benfenati F, Kulozik AE, Valtorta F (2013) Nonsense-mediated mRNA decay and loss-of-function of the protein underlie the X-linked epilepsy associated with the W356X mutation in synapsin I. PLoS ONE 8:e67724
34. Gitler D, Takagishi Y, Feng J, Ren Y, Rodriguez RM, Wetsel WC, Greengard P, Augustine GJ (2004) Different presynaptic roles of synapsin at excitatory and inhibitory synapses. J Neurosci 24:11368–11380
35. Greco B, Managò F, Tucci V, Kao HT, Valtorta F, Benfenati F (2013) Autism-related behavioral abnormalities in synapsin knockout mice. Behav Brain Res 251:65–74
36. Grynkiewicz G, Poenie M, Tsien RY (1985) A new generation of Ca^{2+} indicators with greatly improved fluorescence properties. J Biol Chem 260:3440–3450
37. Gulyás AI, Hájos N, Freund TF (1996) Interneurons containing calretinin are specialized to control other interneurons in the rat hippocampus. J Neurosci 16:3397–3411
38. Guerrini R, Conti V, Mantegazza M, Balestrini S, Galanopoulou AS, Benfenati F (2022) Developmental and epileptic encephalopathies: from genetic heterogeneity to phenotypic continuum. Physiol Rev. Epub ahead of print. https://doi.org/10.1152/physrev.00063.2021
39. Hosaka M, Südhof TC (1998) Synapsin I and II are ATP-binding proteins with differential Ca^{2+} regulation. J Biol Chem 273:1425–1429
40. Hosaka M, Südhof TC (1999) Homo- and heterodimerization of synapsins. J Biol Chem 274:16747–16753
41. Hu H, Gan J, Jonas P (2014) Fast spiking, parvalbumin+ GABAergic interneurons: from cellular design to microcircuit function. Science 345:1255263–1255263
42. Jorgensen WL, Chandrasekhar J, Madura JD, Impey RW, Klein ML (1983) Comparison of simple potential functions for simulating liquid water. J Chem Phys 79:926–935
43. Jovanovic JN, Sihra TS, Nairn AC, Hemmings HC Jr, Greengard P, Czernik AJ (2001) Opposing changes in phosphorylation of specific sites in synapsin I during Ca^{2+}-dependent glutamate release in isolated nerve terminals. J Neurosci 21:7944–7953
44. Kavalali ET (2015) The mechanisms and functions of spontaneous neurotransmitter release. Nat Rev Neurosci 16:5–16
45. Kavalali ET (2020) Neuronal Ca^{2+} signalling at rest and during spontaneous neurotransmission. J Physiol 598:1649–1654
46. Lee SH, Rosenmund C, Schwaller B, Neher E (2000) Differences in Ca^{2+} buffering properties between excitatory and inhibitory hippocampal neurons from the rat. J Physiol 525:405–418
47. Leung A (1994) Fixation. In: Woods AE, Ellis RC (eds) Laboratory histopathology: a complete reference. Churchill Livingstone, New York
48. Li L, Chin LS, Shupliakov O, Brodin L, Sihra TS, Hvalby O, Jensen V, Zheng D, McNamara JO, Greengard P, Anderson P (1995) Impairment of synaptic vesicle clustering and of synaptic transmission, and increased seizure propensity, in synapsin I-deficient mice. Proc Natl Acad Sci USA 92:9235–9239
49. Li M, Wang Y, Banerjee R, Marinelli F, Silberberg S, Faraldo-Gómez JD, Hattori M, Swartz KJ (2019) Molecular mechanisms of human P2X3 receptor channel activation and modulation by divalent cation bound ATP. Elife 8:e47060
50. Longhena F, Faustini G, Brembati V, Pizzi M, Benfenati F, Bellucci A (2021) An updated reappraisal of synapsins: structure, function and role in neurological and psychiatric disorders. Neurosci Biobehav Rev 130:33–60
51. Mackerell AD Jr, Feig M, Brooks CL 3rd (2004) Extending the treatment of backbone energetics in protein force fields: limitations of gas-phase quantum mechanics in reproducing protein conformational distributions in molecular dynamics simulations. J Comput Chem 25:1400–1415
52. Martyna GJ, Tobias DJ, Klein ML (1994) Constant pressure molecular dynamics algorithms. J Chem Phys 101:4177–4189
53. Medrihan L, Cesca F, Raimondi A, Lignani G, Baldelli P, Benfenati F (2013) Synapsin II desynchronizes neurotransmitter release at inhibitory synapses by interacting with presynaptic calcium channels. Nat Commun 4:1512
54. Medrihan L, Ferrea E, Greco B, Baldelli P, Benfenati F (2015) Asynchronous GABA release is a key determinant of tonic inhibition and controls neuronal excitability: a study in the synapsin $II^{-/-}$ mouse. Cereb Cortex 25:3356–3368
55. Michetti C, Caruso A, Pagani M, Sabbioni M, Medrihan L, David G, Galbusera A, Morini M, Gozzi A, Benfenati F, Scattoni ML (2017) The knockout of synapsin II in mice impairs social behavior and functional connectivity generating an ASD-like phenotype. Cereb Cortex 27:5014–5023
56. Michetti C, Falace A, Benfenati F, Fassio A (2022) Synaptic genes and neurodevelopmental disorders: from molecular mechanisms

to developmental strategies of behavioral testing. Neurobiol Dis 173:105856
57. Milovanovic D, De Camilli P (2017) Synaptic vesicle clusters at synapses: a distinct liquid phase? Neuron 93:995–1002
58. Milovanovic D, Wu Y, Bian X, De Camilli P (2018) A liquid phase of synapsin and lipid vesicles. Science 361:604–607
59. Neher E, Sakaba T (2008) Multiple roles of calcium ions in the regulation of neurotransmitter release. Neuron 59:861–872
60. Nguyen DK, Rouleau I, Sénéchal G, Ansaldo AI, Gravel M, Benfenati F, Cossette P (2015) X-linked focal epilepsy with reflex bathing seizures: characterization of a distinct epileptic syndrome. Epilepsia 56:1098–1108
61. Onofri F, Giovedi S, Kao HT, Valtorta F, Bongiorno Borbone L, De Camilli P, Greengard P, Benfenati F (2000) Specificity of the binding of synapsin I to Src homology 3 domains. J Biol Chem 275:29857–29867
62. Orlando M, Lignani G, Maragliano L, Fassio A, Onofri F, Baldelli P, Giovedí S, Benfenati F (2014) Functional role of ATP binding to synapsin I in synaptic vesicle trafficking and release dynamics. J Neurosci 34:14752–14768
63. Orlando M, Schmitz D, Rosenmund C, Herman MA (2019) Calcium-independent exo-endocytosis coupling at small central synapses. Cell Rep 29:3767-3774.e3
64. Pechstein A, Tomilin N, Fredrich K, Vorontsova O, Sopova E, Evergren E, Haucke V, Brodin L, Shupliakov O (2020) Vesicle clustering in a living synapse depends on a synapsin region that 96 mediates phase separation. Cell Rep 30:2594–2602
65. Peron A, Baratang NV, Canevini MP, Campeau PM, Vignoli A (2018) Hot water epilepsy and SYN1 variants. Epilepsia 59:2162–2163
66. Phillips JC, Braun R, Wang W, Gumbart J, Tajkhorshid E, Villa E, Chipot C, Skeel RD, Kalé L, Schulten K (2005) Scalable molecular dynamics with NAMD. J Comput Chem 26:1781–1802
67. Rangaraju V, Calloway N, Ryan TA (2014) Activity-driven local ATP synthesis is required for synaptic function. Cell 156:825–835
68. Rizzoli SO (2014) Synaptic vesicle recycling: steps and principles. EMBO J 33:788–822
69. Rosahl TW, Geppert M, Spillane D, Herz J, Hammer RE, Malenka RC, Südhof TC (1993) Short-term synaptic plasticity is altered in mice lacking synapsin I. Cell 75:661–670
70. Rosahl TW, Spillane D, Missler M, Herz J, Selig DK, Wolff JR, Hammer RE, Malenka RC, Südhof TC (1995) Essential functions of synapsins I and II in synaptic vesicle regulation. Nature 375:488–493
71. Ryckaert JP, Ciccotti G, Berendsen HJC (1977) Numerical integration of the Cartesian equations of motion of a system with constraints and molecular dynamics of n-alkanes. J Comput Phys 23:327–341
72. Schiebler W, Jahn R, Doucet JP, Rothlein J, Greengard P (1986) Characterization of synapsin I binding to small synaptic vesicles. J Biol Chem 261:8383–8390
73. Schneggenburger R, Meyer AC, Neher E (1999) Released fraction and total size of a pool of immediately available transmitter quanta at a calyx synapse. Neuron 23:399–409
74. Schwaller B (2010) Cytosolic Ca^{2+} buffers. Cold Spring Harb Perspect Biol 2:a004051
75. Shulman Y, Stavsky A, Fedorova T, Mikulincer D, Atias M, Radinsky I, Kahn J, Slutsky I, Gitler D (2015) ATP binding to synapsin IIa regulates usage and clustering of vesicles in terminals of hippocampal neurons. J Neurosci 35:985–998
76. Siksou L, Rostaing P, Lechaire JP, Boudier T, Ohtsuka T, Fejtova A, Kao HT, Greengard P, Triller A, Marty S (2007) Three-dimensional architecture of presynaptic terminal cytomatrix. J Neurosci 27:6868–6877
77. Simkus CR, Stricker C (2002) The contribution of intracellular calcium stores to mEPSCs recorded in layer II neurones of rat barrel cortex. J Physiol 545:521–535
78. Spillane DM, Rosahl TW, Südhof TC, Malenka RC (1995) Long-term potentiation in mice lacking synapsins. Neuropharmacology 34:1573–1579
79. Takamori S, Holt M, Stenius K, Lemke EA, Grønborg M, Riedel D, Urlaub H, Schenck S, Brügger B, Ringler P, Müller SA, Rammner B, Gräter F, Hub JS, De Groot BL, Mieskes G, Moriyama Y, Klingauf J, Grubmüller H, Heuser J, Wieland F, Jahn R (2006) Molecular anatomy of a trafficking organelle. Cell 127:831–846
80. Takei Y, Harada A, Takeda S, Kobayashi K, Terada S, Noda T, Takahashi T, Hirokawa N (1995) Synapsin I deficiency results in the structural change in the presynaptic terminals in the murine nervous system. J Cell Biol 131:1789–1800
81. Tremblay R, Lee S, Rudy B (2016) GABAergic interneurons in the neocortex: from cellular properties to circuits. Neuron 91:260–292
82. Valente P, Farisello P, Valtorta F, Baldelli P, Benfenati F (2017) Impaired $GABA_B$-mediated presynaptic inhibition increases excitatory strength and alters short-term plasticity in synapsin knockout mice. Oncotarget 8:90061–90076
83. Verstegen AM, Tagliatti E, Lignani G, Marte A, Stolero T, Atias M, Corradi A, Valtorta F, Gitler D, Onofri F, Fassio A, Benfenati F (2014) Phosphorylation of synapsin I by cyclin-dependent kinase-5 sets the ratio between the resting and recycling pools of synaptic vesicles at hippocampal synapses. J Neurosci 34:7266–7280
84. Xiong J, Duan H, Chen S, Kessi M, He F, Deng X, Zhang C, Yang L, Peng J, Yin F (2021) Familial SYN1 variants related neurodevelopmental disorders in Asian pediatric patients. BMC Med Genomics 14:182